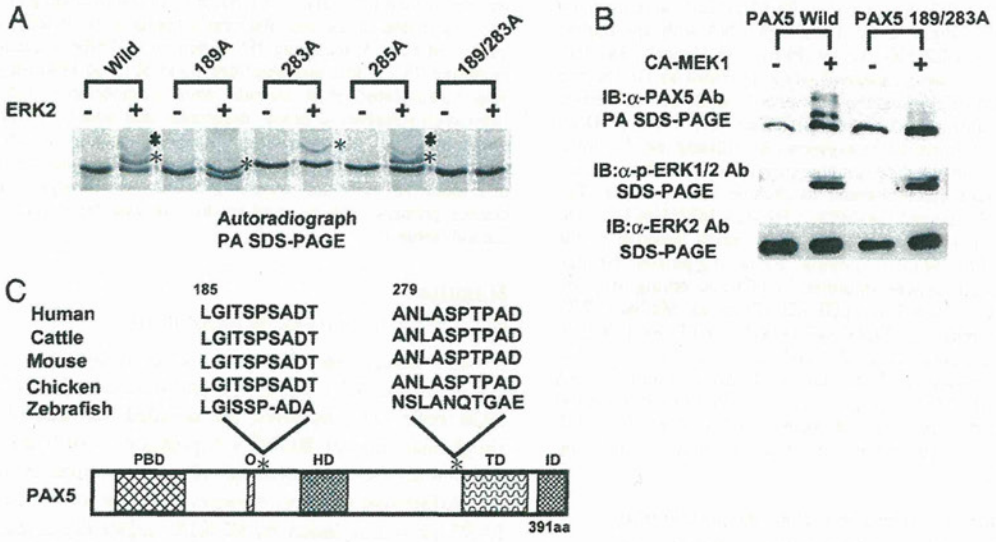

FIGURE 1. PAX5 was phosphorylated by ERK1/2 signal. (**A**) PAX5 was phosphorylated by ERK2 at serines 189 and 283 in vitro. Wild-type PAX5 and PAX5 with the indicated mutations were synthesized in vitro with [^{35}S]-labeling. Mutations are designated by the codon number followed by "A". PAX5 proteins were phosphorylated in vitro with ERK2 and were separated by phosphate-affinity (PA) SDS-PAGE, in which phosphorylated proteins migrate slowly relative to the number of phosphorylation sites. The regular asterisks and bold asterisks indicate PAX5 phosphorylated at one site and two sites, respectively. Mutants of 189A and 283A showed only one shifted band, and all shifted bands disappeared by the mutation of 189/283A, suggesting that serines 189 and 283 were the phosphorylation sites. (**B**) PAX5 was phosphorylated by ERK1/2 in vivo. 293T cells (1×10^5) were transfected with wild-type or mutant PAX5 expression vector (200 ng), with or without cotransfection of constitutively active MEK1 (CA-MEK1) expression vector (200 ng). Cell lysates were separated by PA SDS-PAGE or SDS-PAGE, as indicated, and subjected to immunoblotting (IB). Wild-type PAX5 was phosphorylated by the coexpression of CA-MEK1, but mutant PAX5 was not. (**C**) Conservation of PAX5 phosphorylation sites beyond species. Alignment of amino acid sequences of human, cattle, mouse, chicken, and zebrafish PAX5 corresponding to the phosphorylation sites of human PAX5. Asterisks indicate phosphorylation sites of human PAX5. Amino acid sequences surrounding PAX5 phosphorylation sites are completely conserved, except in zebrafish. HD, Homeobox domain; ID, inhibitory domain; O, conserved octapeptide; PBD, paired box domain; TD, transactivation domain.

occurred at ERK2 phosphorylation sites determined in vitro, we established stable Ramos transfectants of control vector and the expression vectors of wild-type and phosphorylation-defective mutant of PAX5, designated as Control-Ramos, PAX5 Wild-Ramos, and PAX5 189/283A-Ramos, respectively. Because phosphorylation of endogenous PAX5 masked the difference in the phosphorylation status between exogenously expressed wild-type and mutant PAX5 (data not shown), we further introduced the siRNA targeting 3′ UTR of endogenous PAX5 to specifically knockdown endogenous PAX5 of these transfectants. Successful specific knockdown of endogenous PAX5 is demonstrated in Fig. 2B. In this system, BCR signal-induced PAX5 phosphorylation was completely diminished by the mutation at ERK2 phosphorylation sites (Fig. 2C). These results indicated that BCR signal-induced PAX5 phosphorylation was mediated by ERK1/2.

We also performed the same experiment in Fig. 2A using mouse spleen cells that were rich in primary B cells. The results were similar to that in Ramos cells. BCR stimulation of mouse spleen cells induced ERK1/2 phosphorylation and PAX5 phosphorylation, which was inhibited by U0126 (Fig. 2D). These results suggested that PAX5 phosphorylation by ERK1/2 in response to BCR stimulation also occurred in primary normal B cells.

ERK1/2 signal canceled PAX5-dependent transcriptional repression of BLIMP1

Next, we set out to identify the effect of phosphorylation on BLIMP1 repression by PAX5. To replicate BLIMP1 repression by PAX5 in the luciferase assay, we constructed a reporter gene containing an ~2-kbp region of *BLIMP1* promoter, including putative binding sites for PAX5, and NF-κB, one of the BLIMP1 expression activators, according to a previous report (19) (Fig. 3A). Before the assay, we focused on enhancement of PAX5 expression by CA-MEK1 coexpression observed in Fig. 1B, because it may affect the luciferase assay comparing PAX5 function with and without CA-MEK1 coexpression. We judged that this enhancement of PAX5 expression is due to a nonspecific effect of ERK1/2 signal on the transcriptional machinery on the T7 or CMV promoter of PAX5/pCDNA, because CA-MEK1 coexpression also enhanced the expression of the phosphorylation-defective mutant of PAX5 (Fig. 1B), indicating that this phenomenon was independent of PAX5 phosphorylation, and BCR stimulation or CA-MEK1 expression in Ramos cells did not affect the expression level of endogenous PAX5 (Fig. 2A, data not shown). Therefore, we investigated the effect of CA-MEK1 coexpression on PAX5 expression in detail (Supplemental Fig. 2A) and adjusted the amount of PAX5 expression vector used for the luciferase assay when it was cotransfected with the CA-MEK1 expression vector to keep the PAX5 expression level constant. A constant expression of PAX5 among luciferase samples was confirmed by immunoblotting (Fig. 3B, *lower panel*).

Luciferase expression was strongly induced by NF-κB expression, which was decreased to 15% of the control level by wild-type PAX5 coexpression (Fig. 3B, *lane 2* versus *lane 4*). Importantly, CA-MEK1 coexpression increased the luciferase expression suppressed by wild-type PAX5 to 80% of the control level (Fig. 3B, *lane 3* versus *lane 5*), indicating that ERK1/2 signal canceled transcriptional repression by PAX5. Furthermore, transcriptional repression by mutant PAX5 was attenuated by CA-MEK1 coexpression to a significantly lesser extent than that by wild-type PAX5 (Fig. 3B, *lane 5* versus *lane 7*, $p < 0.05$), indicating its resistance to ERK1/2 signal-dependent cancellation of the transcriptional repression. These data suggested that PAX5 phosphorylation by ERK1/2 signal played an important role in the abolition of BLIMP1 repression by PAX5.

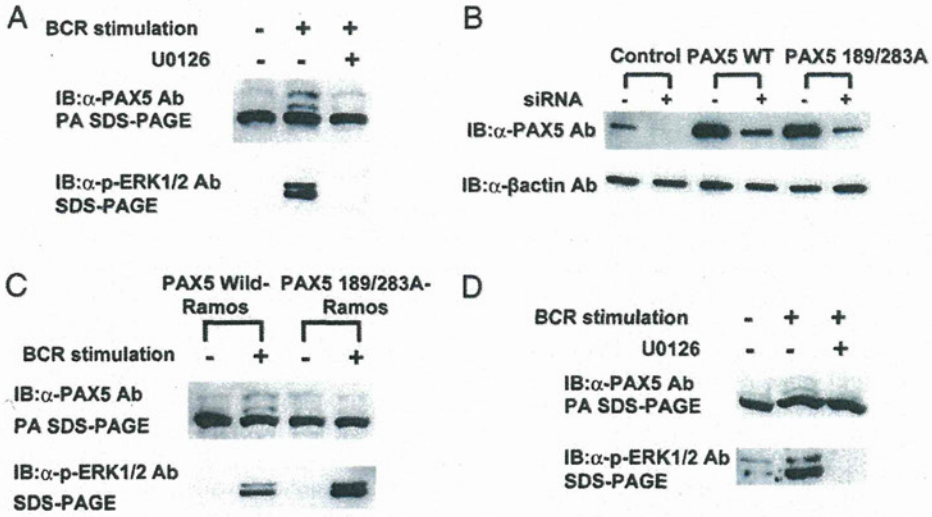

FIGURE 2. PAX5 phosphorylation was induced by BCR stimulation through ERK1/2 signal in B cells. (**A**) MEK1 inhibitor inhibited BCR signal-induced PAX5 phosphorylation. Ramos cells were stimulated with anti-IgM Ab (2 μg/ml) for 10 min. U0126 (10 μM) was added 60 min before stimulation, as indicated. Cell lysates were subjected to immunoblotting analyses, as in Fig. 1B. PAX5 phosphorylation was induced by BCR stimulation, which was inhibited by U0126. (**B**) Specific knockdown of endogenous PAX5 in Ramos cells. The indicated PAX5 stable transfectants of Ramos cells were introduced control siRNA (−) and siRNA targeting the 3′-UTR of endogenous PAX5 (+), as indicated. Twenty-four hours later, cells were lysed and subjected to immunoblotting. Reduction of PAX5 expression by siRNA introduction was much stronger in Control-Ramos cells that expressed only endogenous PAX5 than in PAX5 Wild-Ramos cells and PAX5 189/283A-Ramos cells that expressed endogenous and exogenous PAX5, indicating specific knockdown of endogenous PAX5. (**C**) The mutations at ERK2 phosphorylation sites abolished BCR signal-induced PAX5 phosphorylation. The siRNA targeting the 3′-UTR of endogenous PAX5 mRNA was introduced into PAX5 Wild-Ramos cells and PAX5 189/283A-Ramos cells to knockdown endogenous PAX5 specifically. Then, cells were stimulated with anti-IgM Ab, lysed, and subjected to immunoblotting analyses, as in (A). (**D**) MEK1 inhibitor inhibited BCR signal-induced PAX5 phosphorylation in mouse spleen cells. Mouse spleen cells were treated and analyzed as in (A), except that cells were stimulated with anti-IgM Ab (10 μg/ml) for 10 min.

Of note, mutant PAX5 suppressed the luciferase expression more strongly than did wild-type PAX5 when CA-MEK1 was not coexpressed (Fig. 3B, *lane 4* versus *lane 6*). This is probably due to mild attenuation of wild-type PAX5 ability by weak phosphorylation of PAX5 by constitutively activated ERK1/2 signal in 293T cells, because ERK1/2 was weakly, but constitutively, phosphorylated in 293T cells without CA-MEK1 coexpression (Supplemental Fig. 2B), and administration of U0126 enhanced

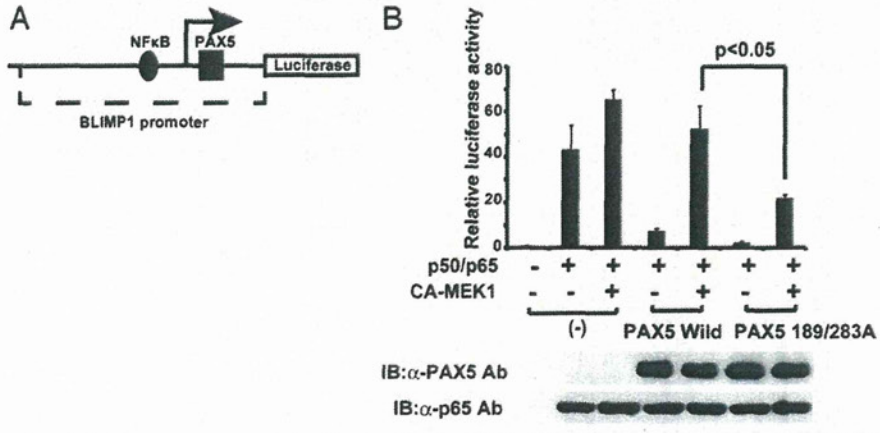

FIGURE 3. PAX5 phosphorylation attenuates transcriptional repression by PAX5. (**A**) Schematic representation of BLIMP1-luc/pGL4, the reporter plasmid for analysis of transcriptional repression by PAX5. The part of the *BLIMP1* promoter (~2 kbp) containing putative NF-κB– and PAX5-binding sequences was subcloned to luciferase reporter plasmid. (**B**) Transcriptional repression by PAX5. Luciferase assay was performed using BLIMP1-luc/pGL4. When CA-MEK1 expression vector was cotransfected, the amount of PAX5 expression vectors was reduced from 100 to 20 ng to avoid elevation of the PAX5 expression level by CA-MEK1 coexpression. Triplicate sets of cells were lysed separately: two sets for the luciferase assay using luciferase assay buffer and the other set for immunoblotting using whole-cell extraction buffer. Luciferase activities in three independent transfection experiments are shown as average values relative to the basal activity observed in control cells (results are the mean ± SD). Cell lysates were also subjected to immunoblotting (IB), as indicated, to confirm the equal expressions of PAX5 (*middle panel*). The expression vectors of NF-κB p50 and p65 were 50 ng each and were not adjusted in cotransfection with CA-MEK1. Equal expressions of NF-κB p65 were also confirmed by immunoblotting (*bottom panel*). Statistical comparisons were performed using the *t* test. Wild-type and mutant PAX5 suppressed NF-κB–induced luciferase expression. Transcriptional repression by wild-type PAX5 was canceled by CA-MEK1 coexpression, whereas that by mutant PAX5 was significantly more resistant to CA-MEK1 coexpression (*lane 5* versus *lane 7*, $p < 0.05$).

the transcriptional repression by wild-type PAX5 but did not affect that by mutant PAX5 and diminished the difference between them (Supplemental Fig. 2C).

BCR signal-induced PAX5 phosphorylation increased BLIMP1 expression in B cells

To further confirm the BLIMP1 derepression by BCR stimulation, we first examined BLIMP1 mRNA expression after BCR stimulation in Ramos cells. BLIMP1 mRNA expression was induced by BCR stimulation following ERK1/2 and PAX5 phosphorylation, and U0126 inhibited the induction of BLIMP1 expression (Fig. 4A). Next, we used Ramos transfectants with specific knockdown of endogenous PAX5. Exogenous expression of wild-type and mutant PAX5 reduced BLIMP1 expression. BCR stimulation relieved BLIMP1 repression by wild-type PAX5, whereas repression by mutant PAX5 was resistant to BCR stimulation (Fig. 4B). These data indicated that BCR signal-induced BLIMP1 expression was mediated by PAX5 phosphorylation by ERK1/2. Notably, in contrast to the luciferase assay in Fig. 3B, no difference in the repression of BLIMP1 was observed between wild-type and mutant PAX5 transfectants of Ramos cells when there was no BCR stimulation (Fig. 4B, *lane 3* versus *lane 5*). This occurs because Ramos cells have no constitutive ERK1/2 activation, which is different from 293T cells (Supplemental Fig. 2B).

We also examined BCR signal-induced BLIMP1 expression in mouse spleen B cells. BCR stimulation of mouse spleen B cells induced BLIMP1 mRNA expression, which was inhibited by U0126 (Fig. 4C). Taken together with BCR signal-induced PAX5 phosphorylation in these cells (Fig. 2D), these data implied that BCR signal-induced BLIMP1 derepression through PAX5 phosphorylation by ERK1/2 might also occur in primary B cells.

PAX5 phosphorylation did not affect DNA-binding ability or cellular localization

To clarify how PAX5 phosphorylation attenuated its function, we used EMSA to investigate the effect of PAX5 phosphorylation on DNA-binding ability. PAX5, synthesized in vitro, was incubated with radiolabeled oligomers containing the PAX5-binding sequence in the *CD19* promoter. The obtained single band was competed by the presence of a 200-fold molar excess of non-radiolabeled oligomers and was supershifted by anti-PAX5 Ab but not by control rabbit IgG (Fig. 5A). Wild-type and mutant PAX5 were subjected to in vitro kination, with or without ERK2, and then to EMSA. No difference in DNA-binding activity was observed, regardless of phosphorylation by ERK2 and phosphorylation-defective mutation (Fig. 5A). These results indicated that PAX5 phosphorylation did not affect its DNA-binding ability.

Next, we examined the alteration of PAX5 cellular localization by coexpression of CA-MEK1 or phosphorylation-defective mutation. Overexpressed wild-type and mutant PAX5 localized diffusely in the nucleus, and this was not affected by coexpression of CA-MEK1, suggesting that cellular localization of PAX5 was not altered by its phosphorylation (Fig. 5B). The molecular mecha-

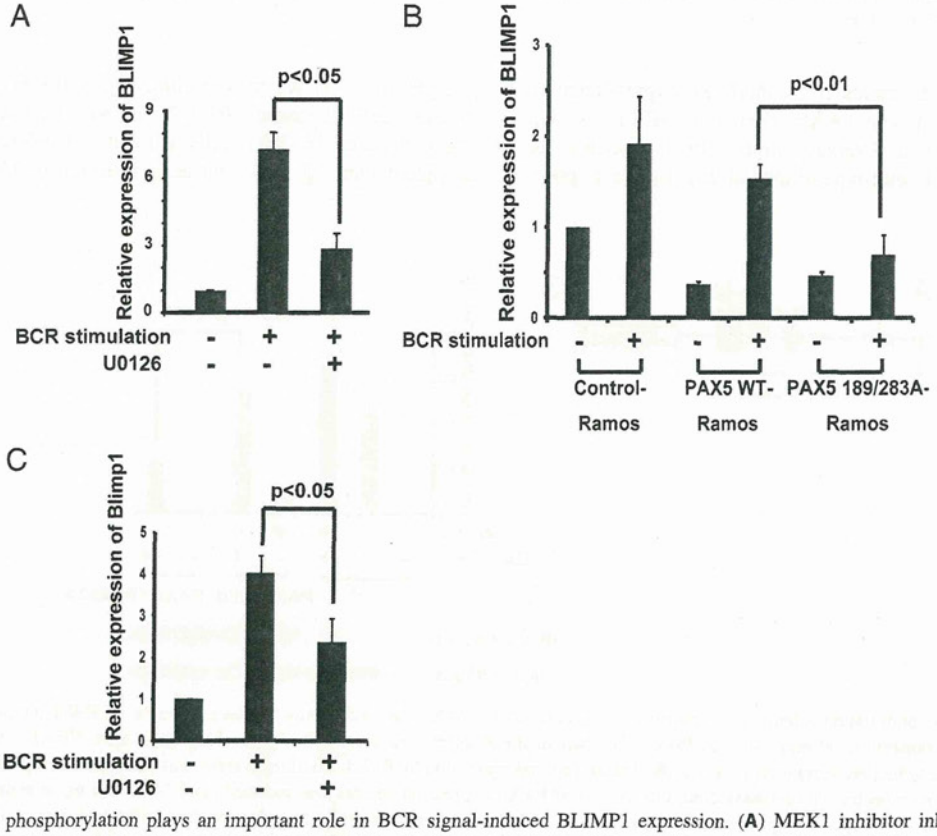

FIGURE 4. PAX5 phosphorylation plays an important role in BCR signal-induced BLIMP1 expression. (**A**) MEK1 inhibitor inhibited BCR signal-induced BLIMP1 expression. Ramos cells were treated as in Fig. 2A. Eight hours after stimulation, RNA was harvested, and mRNA expression of BLIMP1 was quantified by real-time RT-PCR. The relative mRNA expression levels reflect duplicate values from two independent experiments. Statistical comparisons were performed by using the *t* test. (**B**) Phosphorylation-defective mutant of PAX5 abolished BCR signal-induced BLIMP1 expression. Control-Ramos, PAX5 Wild-Ramos, and PAX5 189/283A-Ramos cells were introduced siRNA for specific knockdown of endogenous PAX5 and stimulated with anti-IgM Ab for BCR stimulation as in Fig. 2C. RNA harvest and quantification of BLIMP1 mRNA were performed as in (A). (**C**) MEK1 inhibitor inhibited BCR signal-induced BLIMP1 expression in mouse spleen B cells. Mouse spleen B cells, purified as described in *Materials and Methods*, were treated and analyzed as in (A), except that cells were stimulated with anti-IgM Ab (10 μg/ml), and RNA extraction was performed 1 h after stimulation.

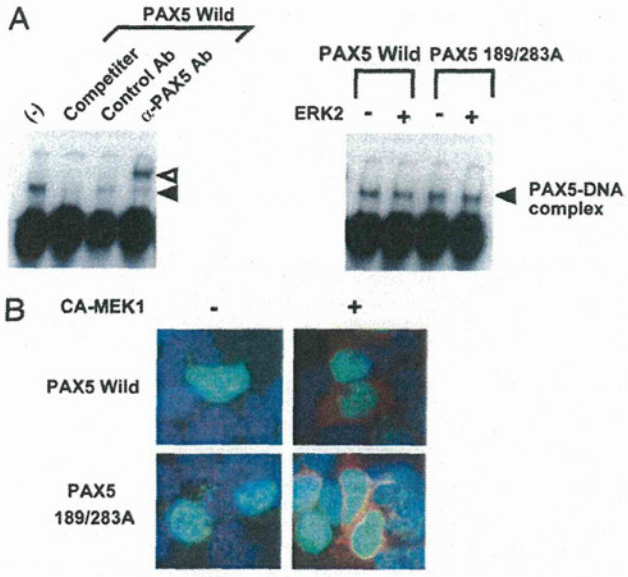

FIGURE 5. PAX5 phosphorylation did not affect DNA-binding ability or cellular localization. (**A**) Phosphorylation of PAX5 did not affect DNA-binding ability. Equal amounts of PAX5 synthesized in vitro were incubated with ^{32}P-labeled oligonucleotide probe containing the PAX5-binding sequence of the *CD19* promoter in the presence or absence of a 200-fold molar excess of unlabeled oligonucleotide (competitor), normal rabbit IgG (control Ab), or anti-PAX5 Ab (*left panel*). PAX5–DNA complex (black arrowhead) was visualized with an imaging analyzer. Supershifted band is indicated by the white arrowhead. Equal amounts of wild-type and mutant PAX5 were first subjected to in vitro phosphorylation, with or without ERK2, and then applied to EMSA (*right panel*). DNA-binding ability of PAX5 was not affected by phosphorylation. (**B**) Phosphorylation of PAX5 did not affect its localization. 293T cells were transfected with the expression vectors for wild-type and mutant PAX5, with or without HA-tagged CA-MEK1. Localization of PAX5 was observed with immunofluorescence staining using anti-PAX5 Ab with Alexa Fluor 488-conjugated secondary Ab (green), anti-HA Ab with Alexa Fluor 568-conjugated secondary Ab (red), and DAPI (blue). Original magnification ×400. Diffuse nuclear localization of PAX5 was not affected by the coexpression of HA-tagged CA-MEK1 or phosphorylation site mutations.

nisms through which PAX5 phosphorylation abolishes transcriptional repression of BLIMP1 are unknown.

Discussion

The data presented in this article support our speculation that PAX5 phosphorylation by ERK1/2 negatively affected BLIMP1 repression by PAX5. It is reported that BLIMP1 repression by PAX5 is abolished after BCR stimulation by Ag. Once BLIMP1 is expressed, it suppresses PAX5, which allows greater expression of BLIMP1. This positive feedback loop enables quick replacement of PAX5 with BLIMP1, which initiates plasma cell differentiation (14). Kallies et al. (16) investigated the first event of plasma cell differentiation in detail; they reported that the abolition of PAX5-mediated repression of BLIMP1 was the first event to initiate plasma cell differentiation and that the mechanism was neither a decrease in the DNA-binding ability of PAX5 nor downregulation of the PAX5 expression level and was yet to be revealed. PAX5 phosphorylation by ERK1/2 could be a clue to this uncertainty. The schema of this putative model is shown in Fig. 6.

It should be noted that Ramos cells or primary B cells from mouse spleen did not undergo plasma cell differentiation as the result of BCR stimulation with anti-IgM Ab (data not shown), despite the stimulation-induced phosphorylation of ERK1/2 and PAX5 and BLIMP1 expression. We could not keep the primary B cells alive for longer than a few days and could not estimate the differentiation. With regard to Ramos cells, one possible reason is that ERK1/2 phosphorylation induced by anti-IgM Ab stimulation was transient, peaking 10 min after stimulation and returning to basal levels ~2 h later. The kinetics of PAX5 phosphorylation were similar to those of ERK1/2 phosphorylation and, consistent with these kinetics, BLIMP1 mRNA expression was also transient and returned to the basal level within 24 h (data not shown). After anti-IgM Ab stimulation, BLIMP1 expression in Ramos cells is not sufficient to suppress PAX5 and initiate the above-described positive-feedback loop to replace PAX5 with BLIMP1. BCR stimulation with Ag is not the only stimulation required for plasma cell differentiation. Stimulation with cytokines, such as IL-2, IL-4, IL-10, and IL-21, and contact-dependent engagement of CD40 on B cells by CD40L (CD154), expressed by activated CD4$^+$ T cells, are required for plasma differentiation (22–26). Costimulation with these cytokines and T cells might prolong and enhance ERK1/2 phosphorylation and PAX5 phosphorylation and enable enough BLIMP1 expression to initiate plasma cell differentiation. The other possible reason is that Ramos cells, a lymphoma cell line, have impaired differentiation, as do tumor cells. BLIMP1 expression is induced by the cooperation of transcription factors, such as STAT3, IRF-4, and NF-κB (27, 28). Normal GCB cells express these factors properly and are ready to respond to BCR stimulation, which might enable a rapid and substantial increase in BLIMP1 expression in response to even transient PAX5 phosphorylation.

Other researchers reported the phosphorylation of PAX family proteins by the MAPK superfamily. PAX2 is phosphorylated by JNK at the transactivation domain (29), and both ERK1/2 and

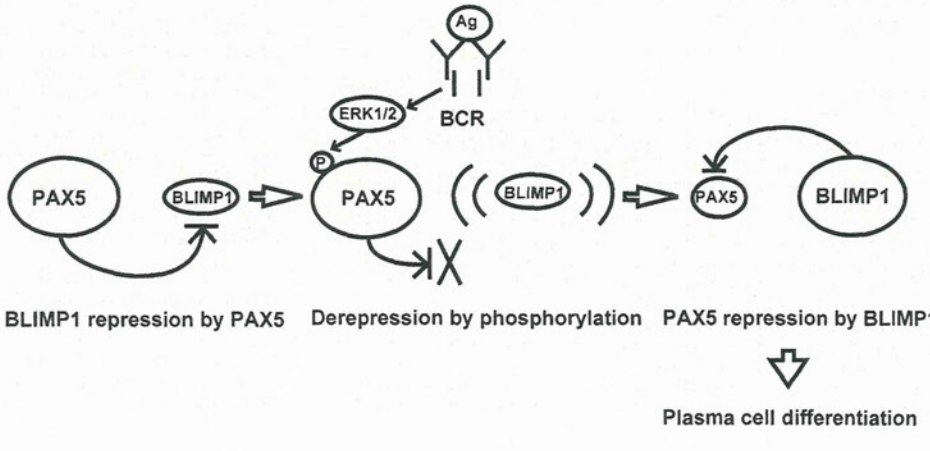

FIGURE 6. Putative schematic model of plasma cell differentiation triggered by PAX5 phosphorylation. PAX5 represses BLIMP1 expression during B cell development (*left*). When BCR signal is induced by Ag, ERK1/2 signal activation and PAX5 phosphorylation occur simultaneously, and repression of BLIMP1 is attenuated by PAX5 phosphorylation (*middle*). Once BLIMP1 is expressed, it suppresses PAX5 (*right*). Finally, PAX5 is replaced with BLIMP1, and plasma cell differentiation is initiated.

p38 phosphorylate PAX6 at the same sites: serines 376 and 413 and threonine 323 (30). This phosphorylation enhances the transcriptional activities of PAX family proteins. In addition, PAX6 phosphorylation by homeodomain-interacting protein kinase 2 (31), sumoylation of PAX6 (32), and acetylation of PAX5 by p300 (33) are reported to be posttranslational modifications of PAX family proteins, and all enhance the transactivation of PAX family proteins; therefore, negative regulation of PAX5 function by phosphorylation seems to be unique. Serines of PAX5 phosphorylation sites are not conserved in any other PAX family proteins. PAX5 is the only PAX family protein that regulates the differentiation of hematopoietic cells and might obtain a unique method to respond to extracellular signals. Furthermore, the cancellation of PAX family-dependent transcriptional repression by phosphorylation may also be unique to PAX5, although the effect of phosphorylation on transcriptional repression by other members of the PAX family has not been investigated.

The aberrant expression of normal PAX5 protein by the fusion gene between the potent enhancer of the *IGH* gene and the *PAX5* promoter was found in non-Hodgkin's lymphoma patients with the chromosomal translocation, t(9;14)(p13;q32) (34, 35). The oncogenicity of this fusion gene might be explained by impaired initiation of plasma cell differentiation due to sustained repression of BLIMP1 by overexpressed PAX5. Similarly, phosphorylation-defective mutation of PAX5 might impair plasma cell differentiation and cause lymphoma; therefore, we examined the genome DNA sequence surrounding PAX5 phosphorylation sites in 85 cases of diffuse large B cell lymphoma, but no mutation was found (data not shown; information on samples and sequencing methods is described in *Materials and Methods*). PAX5 mutations in lymphoma cells, if they exist, might be at the ERK1/2 binding site of PAX5, which is currently unknown.

In summary, our study provides evidence for an ERK1/2 pathway that phosphorylates PAX5 in response to BCR stimulation; this increase in PAX5 phosphorylation may associate with attenuated transcriptional repression by PAX5, derepression of BLIMP1, and initiation of plasma cell differentiation. This work provides new insight into the regulation of PAX5 function and establishes a novel relationship among the BCR signal, ERK1/2, and PAX5.

Acknowledgments

We thank Tomoko Kawake, Yoko Matsuyama, Asako Watanabe, and Chika Wakamatsu for technical assistance.

Disclosures

T.N. received research funding from Otsuka Pharmaceutical Co., Ltd., Kyowa Hakko Kirin Co., Ltd., Wyeth, and Chugai Pharmaceutical Co., Ltd. K.S. is a graduate student at Nagoya University and an employee of Otsuka Pharmaceutical Co., Ltd.

References

1. Nutt, S. L., A. M. Morrison, P. Dörfler, A. Rolink, and M. Busslinger. 1998. Identification of BSAP (Pax-5) target genes in early B-cell development by loss- and gain-of-function experiments. *EMBO J.* 17: 2319–2333.
2. Busslinger, M. 2004. Transcriptional control of early B cell development. *Annu. Rev. Immunol.* 22: 55–79.
3. Mikkola, I., B. Heavey, M. Horcher, and M. Busslinger. 2002. Reversion of B cell commitment upon loss of Pax5 expression. *Science* 297: 110–113.
4. Nutt, S. L., D. Eberhard, M. Horcher, A. G. Rolink, and M. Busslinger. 2001. Pax5 determines the identity of B cells from the beginning to the end of B-lymphopoiesis. *Int. Rev. Immunol.* 20: 65–82.
5. Kozmik, Z., S. Wang, P. Dörfler, B. Adams, and M. Busslinger. 1992. The promoter of the CD19 gene is a target for the B-cell-specific transcription factor BSAP. *Mol. Cell. Biol.* 12: 2662–2672.
6. Maier, H., R. Ostraat, S. Parenti, D. Fitzsimmons, L. J. Abraham, C. W. Garvie, and J. Hagman. 2003. Requirements for selective recruitment of Ets proteins and activation of mb-1/Ig-alpha gene transcription by Pax-5 (BSAP). *Nucleic Acids Res.* 31: 5483–5489.
7. Schebesta, M., P. L. Pfeffer, and M. Busslinger. 2002. Control of pre-BCR signaling by Pax5-dependent activation of the BLNK gene. *Immunity* 17: 473–485.
8. Morrison, A. M., S. L. Nutt, C. Thévenin, A. Rolink, and M. Busslinger. 1998. Loss- and gain-of-function mutations reveal an important role of BSAP (Pax-5) at the start and end of B cell differentiation. *Semin. Immunol.* 10: 133–142.
9. Souabni, A., C. Cobaleda, M. Schebesta, and M. Busslinger. 2002. Pax5 promotes B lymphopoiesis and blocks T cell development by repressing Notch1. *Immunity* 17: 781–793.
10. Holmes, M. L., S. Carotta, L. M. Corcoran, and S. L. Nutt. 2006. Repression of Flt3 by Pax5 is crucial for B-cell lineage commitment. *Genes Dev.* 20: 933–938.
11. Usui, T., Y. Wakatsuki, Y. Matsunaga, S. Kaneko, H. Koseki, and T. Kita. 1997. Overexpression of B cell-specific activator protein (BSAP/Pax-5) in a late B cell is sufficient to suppress differentiation to an Ig high producer cell with plasma cell phenotype. [Published erratum appears in 1999 *J. Immunol.* 163: 1091.] *J. Immunol.* 158: 3197–3204.
12. Reimold, A. M., P. D. Ponath, Y. S. Li, R. R. Hardy, C. S. David, J. L. Strominger, and L. H. Glimcher. 1996. Transcription factor B cell lineage-specific activator protein regulates the gene for human X-box binding protein 1. *J. Exp. Med.* 183: 393–401.
13. Wang, L. D., and M. R. Clark. 2003. B-cell antigen-receptor signalling in lymphocyte development. *Immunology* 110: 411–420.
14. Lin, K. I., C. Angelin-Duclos, T. C. Kuo, and K. Calame. 2002. Blimp-1-dependent repression of Pax-5 is required for differentiation of B cells to immunoglobulin M-secreting plasma cells. *Mol. Cell. Biol.* 22: 4771–4780.
15. Calame, K. L., K. I. Lin, and C. Tunyaplin. 2003. Regulatory mechanisms that determine the development and function of plasma cells. *Annu. Rev. Immunol.* 21: 205–230.
16. Kallies, A., J. Hasbold, K. Fairfax, C. Pridans, D. Emslie, B. S. McKenzie, A. M. Lew, L. M. Corcoran, P. D. Hodgkin, D. M. Tarlinton, and S. L. Nutt. 2007. Initiation of plasma-cell differentiation is independent of the transcription factor Blimp-1. *Immunity* 26: 555–566.
17. Kurahashi, S., F. Hayakawa, Y. Miyata, T. Yasuda, Y. Minami, S. Tsuzuki, A. Abe, and T. Naoe. 2011. PAX5-PML acts as a dual dominant-negative form of both PAX5 and PML. *Oncogene* 30: 1822–1830.
18. Hayakawa, F., and M. L. Privalsky. 2004. Phosphorylation of PML by mitogen-activated protein kinases plays a key role in arsenic trioxide-mediated apoptosis. *Cancer Cell* 5: 389–401.
19. Morgan, M. A., E. Magnusdottir, T. C. Kuo, C. Tunyaplin, J. Harper, S. J. Arnold, K. Calame, E. J. Robertson, and E. K. Bikoff. 2009. Blimp-1/Prdm1 alternative promoter usage during mouse development and plasma cell differentiation. *Mol. Cell. Biol.* 29: 5813–5827.
20. Hayakawa, F., M. Towatari, Y. Ozawa, A. Tomita, M. L. Privalsky, and H. Saito. 2004. Functional regulation of GATA-2 by acetylation. *J. Leukoc. Biol.* 75: 529–540.
21. Yasuda, T., K. Kometani, N. Takahashi, Y. Imai, Y. Aiba, and T. Kurosaki. 2011. ERKs induce expression of the transcriptional repressor Blimp-1 and subsequent plasma cell differentiation. *Sci. Signal.* 4: ra25.
22. Splawski, J. B., D. F. Jelinek, and P. E. Lipsky. 1989. Immunomodulatory role of IL-4 on the secretion of Ig by human B cells. *J. Immunol.* 142: 1569–1575.
23. Kuchen, S., R. Robbins, G. P. Sims, C. Sheng, T. M. Phillips, P. E. Lipsky, and R. Ettinger. 2007. Essential role of IL-21 in B cell activation, expansion, and plasma cell generation during CD4+ T cell-B cell collaboration. *J. Immunol.* 179: 5886–5896.
24. Jelinek, D. F., J. B. Splawski, and P. E. Lipsky. 1986. The roles of interleukin 2 and interferon-gamma in human B cell activation, growth and differentiation. *Eur. J. Immunol.* 16: 925–932.
25. Itoh, K., T. Inoue, K. Ito, and S. Hirohata. 1994. The interplay of interleukin-10 (IL-10) and interleukin-2 (IL-2) in humoral immune responses: IL-10 synergizes with IL-2 to enhance responses of human B lymphocytes in a mechanism which is different from upregulation of CD25 expression. *Cell. Immunol.* 157: 478–488.
26. Good, K. L., V. L. Bryant, and S. G. Tangye. 2006. Kinetics of human B cell behavior and amplification of proliferative responses following stimulation with IL-21. *J. Immunol.* 177: 5236–5247.
27. Kwon, H., D. Thierry-Mieg, J. Thierry-Mieg, H. P. Kim, J. Oh, C. Tunyaplin, S. Carotta, C. E. Donovan, M. L. Goldman, P. Tailor, et al. 2009. Analysis of interleukin-21-induced Prdm1 gene regulation reveals functional cooperation of STAT3 and IRF4 transcription factors. *Immunity* 31: 941–952.
28. Johnson, K., M. Shapiro-Shelef, C. Tunyaplin, and K. Calame. 2005. Regulatory events in early and late B-cell differentiation. *Mol. Immunol.* 42: 749–761.
29. Cai, Y., M. S. Lechner, D. Nihalani, M. J. Prindle, L. B. Holzman, and G. R. Dressler. 2002. Phosphorylation of Pax2 by the c-Jun N-terminal kinase and enhanced Pax2-dependent transcription activation. *J. Biol. Chem.* 277: 1217–1222.
30. Mikkola, I., J. A. Bruun, G. Bjorkoy, T. Holm, and T. Johansen. 1999. Phosphorylation of the transactivation domain of Pax6 by extracellular signal-regulated kinase and p38 mitogen-activated protein kinase. *J. Biol. Chem.* 274: 15115–15126.
31. Kim, E. A., Y. T. Noh, M. J. Ryu, H. T. Kim, S. E. Lee, C. H. Kim, C. Lee, Y. H. Kim, and C. Y. Choi. 2006. Phosphorylation and transactivation of Pax6 by homeodomain-interacting protein kinase 2. *J. Biol. Chem.* 281: 7489–7497.
32. Yan, Q., L. Gong, M. Deng, L. Zhang, S. Sun, J. Liu, H. Ma, D. Yuan, P. C. Chen, X. Hu, et al. 2010. Sumoylation activates the transcriptional activity of Pax-6, an important transcription factor for eye and brain development. *Proc. Natl. Acad. Sci. USA* 107: 21034–21039.

33. He, T., S. Y. Hong, L. Huang, W. Xue, Z. Yu, H. Kwon, M. Kirk, S. J. Ding, K. Su, and Z. Zhang. 2011. Histone acetyltransferase p300 acetylates Pax5 and strongly enhances Pax5-mediated transcriptional activity. *J. Biol. Chem.* 286: 14137–14145.
34. Iida, S., P. H. Rao, P. Nallasivam, H. Hibshoosh, M. Butler, D. C. Louie, V. Dyomin, H. Ohno, R. S. Chaganti, and R. Dalla-Favera. 1996. The t(9;14) (p13;q32) chromosomal translocation associated with lymphoplasmacytoid lymphoma involves the PAX-5 gene. *Blood* 88: 4110–4117.
35. Busslinger, M., N. Klix, P. Pfeffer, P. G. Graninger, and Z. Kozmik. 1996. Deregulation of PAX-5 by translocation of the Emu enhancer of the IgH locus adjacent to two alternative PAX-5 promoters in a diffuse large-cell lymphoma. *Proc. Natl. Acad. Sci. USA* 93: 6129–6134.

Leukemia Research Reports 2 (2013) 21–25

Contents lists available at SciVerse ScienceDirect

Leukemia Research Reports

journal homepage: www.elsevier.com/locate/lrr

Brief Communication

GATA2 zinc finger 2 mutation found in acute myeloid leukemia impairs myeloid differentiation

Keiko Niimi, Hitoshi Kiyoi*, Yuichi Ishikawa, Fumihiko Hayakawa, Shingo Kurahashi, Rika Kihara, Akihiro Tomita, Tomoki Naoe

Department of Hematology and Oncology, Nagoya University Graduate School of Medicine, 65 Tsurumai-cho, Showa-ku, Nagoya 466-8550, Japan

ARTICLE INFO

Article history:
Received 27 November 2012
Received in revised form
4 February 2013
Accepted 12 February 2013

Keywords:
GATA2
AML
Mutation
Differentiation

ABSTRACT

We identified two novel *GATA2* mutations in acute myeloid leukemia (AML). One mutation (p.R308P-GATA2) was a R308P substitution within the zinc finger (ZF)-1 domain, and the other (p.A350_N351ins8-GATA2) was an eight-amino-acid insertion between A350 and N351 residues within the ZF-2 domain. p.R308P-GATA2 did not affect DNA-binding and transcriptional activities, while p.A350_N351ins8-GATA2 reduced them, and impaired G-CSF-induced granulocytic differentiation of 32D cells. Although p.A350_N351ins8-GATA2 did not show a dominant-negative effect over wild-type (Wt)–GATA2 by the reporter assay, it might be involved in the pathophysiology of AML by impairing myeloid differentiation because of little Wt-GATA2 expression in primary AML cells harboring the p.A350_N351ins8 mutation.

1. Introduction

GATA transcription factors contribute to the regulation of cell lineage commitment and differentiation.[1] Although hematopoiesis is controlled by numerous transcription and signaling factors with tightly integrated functions, GATA1, GATA2 and GATA3 in the GATA family are involved in the developmental regulation of hematopoiesis. In addition to the essential role in normal hematopoiesis, recent studies demonstrated that mutation of *GATA* genes is involved in the development and progression of leukemia. p.L359V mutation of *GATA2* gene was identified in about 10% of chronic myeloid leukemia (CML) cases at accelerated phase and myeloid blast crisis.[2] Moreover, recent studies demonstrated that *GATA2* gene mutations were identified in AML patients and in three different familial syndromes characterized by predisposition to myelodysplastic syndrome (MDS) and AML.[3–5] These results collectively indicate that dysregulation of GATA2 might be involved in the development and/or progression of AML.

In this study, we analyzed the biological effects of two novel *GATA2* mutations, which were identified in adult *de novo* AML patients.

2. Materials and methods

The diagnosis of AML was based on the morphology, histopathology, the expression of leukocyte differentiation antigens and/or the French–American–British (FAB) classification. *GATA2* mutation was screened in 96 newly diagnosed *de novo* AML adult patients. Informed consent was obtained from all patients to use their samples for banking and molecular analysis, and approval was obtained from the ethics committee of Nagoya University School of Medicine.

The full-length human wild-type (Wt)- and mutated (Mt)-GATA2 cDNAs were amplified from Wt- or Mt-GATA2-expressing leukemia cells, respectively. C-terminally Myc-tagged GATA2 cDNAs were cloned into pcDNA3.1 vector, and electrophoretic mobility shift assay (EMSA) and luciferase assay were performed as previously reported.[6]

C-terminally Myc-tagged Wt- and mutant-GATA2 cDNAs cloned in the pMX-IP vector were transduced into murine IL3-dependent myeloid progenitor cell line 32D cells as previously described.[7] Stable Wt- and mutant-GATA2-expressing 32D cells were subjected to immunofluorescence, proliferation and differentiation analyses.

Wt- and mutant-GATA2-expressed 32D cells were suspended in RPMI1640 medium containing 10% FCS with an increasing concentration of murine IL3 (R&D Systems), and 2×10^4 cells per well were seeded in 96-well culture plates. Cell viability was measured using the CellTiter96 Proliferation Assay (Promega). For the induction of myeloid differentiation, Wt- and mutant-GATA2-expressed 32D cells were cultured in RPMI1640 medium containing 10% FCS and 30 ng/ml recombinant G-CSF (Kyowa-Kirin, Tokyo, Japan) without IL3.

Luciferase assay and cell proliferation and differentiation analyses were performed three times independently. Differences in continuous variables were analyzed with unpaired *t* test for the

* Corresponding author. Tel.: +81 52 744 2141; fax: +81 52 744 2157.
E-mail address: kiyoi@med.nagoya-u.ac.jp (H. Kiyoi).

2213-0489/$ - see front matter © 2013 Elsevier Ltd. All rights reserved.
http://dx.doi.org/10.1016/j.lrr.2013.02.002

distribution between two groups using Prism 5 (GraphPad Software Inc., La Jolla, CA). For all analyses, the *P* values were two-tailed, and a P value < 0.05 was considered significant.

3. Results

We identified two *GATA2* gene mutations. One mutation (p.R308P-GATA2) was a p.Arg308Pro substitution within the N-terminal zinc finger (ZF)-1 domain in a FAB M6 patient (Fig. 1A and B). The other mutation (p.A350_N351ins8-GATA2) was a 24-nucleotide insertion resulting in an eight-amino-acid insertion between A350 and N351 residues within the C-terminal ZF-2 domain in a FAB M1 patient. This insertion mutation consisted of a one nucleotide insertion and a 23-nucleotide corresponding to N337-R344 residues duplication (Fig. 1A and C). In both patients, each *GATA2* mutation was heterozygous. Unfortunately, we could not analyze germ-line sequence of both patients because of the lack of appropriate material. Therefore, we could not completely determine whether identified mutations were somatic or germ-line mutations.

Both patients revealed normal karyotype and no mutation in *FLT3*, *KIT*, *NRAS*, *TP53*, *NPM1*, *CEBPA*, *RUNX1*, *MLL-PTD* and *IDH1/2* genes.

The expression ratios of Wt- and Mt-GATA2 transcripts of AML cells harboring the p.A350_N351ins8 mutation were semi-quantitatively examined using a gene scanning system with fluorescent-labeled PCR product. Although the p.A350_N351ins8 mutation was heterozygous, little expression of Wt-GATA transcript was observed in the primary AML cells (Fig. 1D).

We transiently expressed Wt- and mutant-GATA2 in 293T cells, and nuclear lysates were extracted 48 h later. In EMSA using an oligonucleotide containing GATA recognition sites, DNA-binding activity of p.A350_N351ins8-GATA2 was reduced to about 40% of that of Wt-GATA2, although that of p.R308P-GATA2 was almost the same as that of Wt-GATA2 (Fig. 2A). Consistent with the DNA-binding activity, the transcriptional activity of p.A350_N351ins8-GATA2 was significantly lower than that of Wt-GATA2 ($P=0.006$), while that of p.R308P-GATA2 was not affected ($P=0.11$) (Fig. 2B). Upon co-expression of Wt-GATA2 with p.A350_N351ins8-GATA2 at a 1:1 ratio, the transcriptional activity of Wt-GATA2 was not affected by p.A350_N351ins8-GATA, indicating that p.A350_N351ins8-GATA2 did not have a dominant-negative effect over Wt-GATA2 (Fig. 2C).

We established Wt- and two Mt- (p.R308P and p.A350_N351ins8)-GATA2-expressing 32D cells to analyze the cellular effects of Mt-GATA2 (Fig. 3A). Immunofluorescence analysis revealed that Mt-GATA2 showed similar localization in the nucleus as Wt-GATA2 (Fig. 3B). Both Wt- and mutant-GATA2-expressing 32D cells did not show autonomous proliferation without the presence of IL3. Furthermore, there was no difference of proliferation abilities at lower concentrations of IL3 between them, indicating that mutant GATA2 did not provide a growth advantage (Fig. 3C). Since mutant GATA2 did not affect the proliferation ability, we examined the G-CSF-mediated granulocytic differentiation in Wt- and Mt-GATA2-expressing 32D cells. Mock- and Wt-GATA2-expressing 32D cells were differentiated to mature neutrophils in the culture with G-CSF for 10 days, while Wt-GATA2 overexpression moderately impaired the granulocytic differentiation. In p.R308P-GATA2-expressing 32D cells, mature neutrophil counts and promyelocyte to neutrophil counts were significantly lower than those of Wt-GATA2-expressing 32D cells after the 10-day culture ($P=0.020$ and $P=0.003$, respectively), while promyelocyte to neutrophil counts were the same after the 14-day culture. However, in p.A350_N351ins8-GATA2-expressing

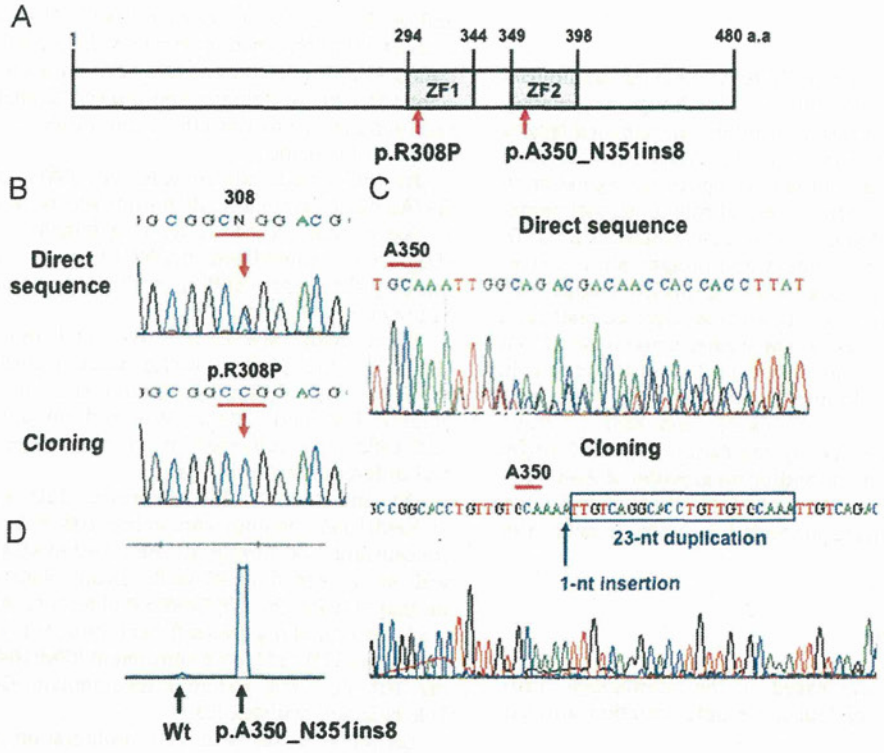

Fig. 1. GATA2 mutations identified in AML. (A) Two novel GATA2 mutations that were identified are shown in the domain structure of GATA2. Two zinc finger domains are indicated by ZF-1 and ZF-2. (B) The sequence diagram of p.R308P mutation. The upper and lower panels show the direct-sequence result and the sequence result after cloning procedure, respectively. (C) The sequence diagram of p.A350_N351ins8 mutation. The upper and lower panels show the direct-sequence result and the sequence result after cloning procedure, respectively. (D) Expression ratio of Wt- and p.A350_N351ins8-GATA2 transcripts of primary AML cells. Little expression of Wt-GATA transcript was observed in the primary AML cells.

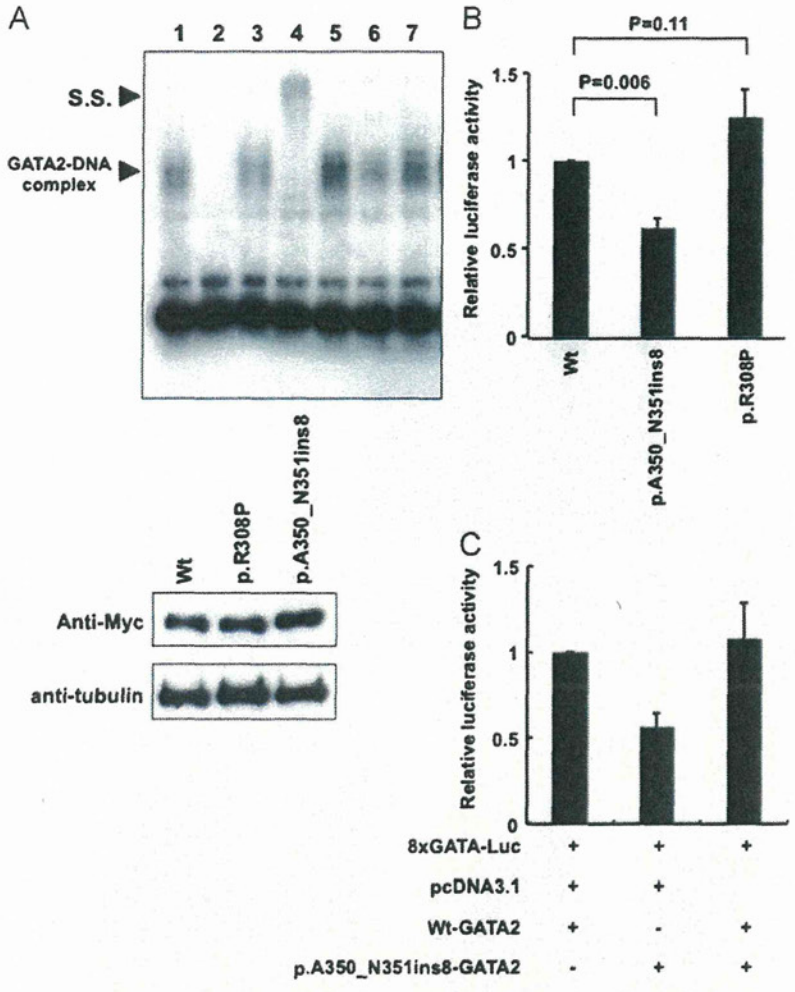

Fig. 2. DNA-binding and transcriptional activities of mutant GATA2. (A) The DNA-binding activities of Wt- and Mt-GATA2 were evaluated by EMSA using an oligonucleotide containing GATA recognition sites. Wt-GATA2 showed the GATA2-DNA complex band (lanes 1 and 5). This band was competed by a 200-fold excess of the unlabeled oligonucleotide (lane 2), and was super-shifted by the addition of anti-GATA2 antibody (lane 4), but not control IgG (lane 3). DNA-binding activity of p.A350_N351ins8-GATA2 was reduced to about 40% of that of Wt-GATA2 (lane 6). In contrast, p.R308P-GATA2 showed almost the same DNA-binding activity as Wt-GATA2 (lane 7). Lower panel shows expression levels of Wt- and Mt-GATA2 proteins in 293 T cells. (B) Transcription activities of Wt- and Mt-GATA2 were evaluated by luciferase reporter assay. 293 T cells were transfected with Wt- or Mt-GATA2 cloned pcDNA3.1 vectors together with a luciferase reporter plasmid containing eight GATA consensus motifs. The transcription activity of p.A350_N351ins8-GATA2 was significantly lower than that of Wt-GATA2 ($P=0.006$), while that of p.R308P-GATA2 was not affected. Mean ± SEM of three independent analyses are shown. (C) Upon co-expression of Wt-GATA2 with p.A350_N351ins8-GATA2 at a 1:1 ratio, the transcriptional activity of Wt-GATA2 was not affected by p.A350_N351ins8-GATA2, indicating that p.A350_N351ins8-GATA2 did not have a dominant-negative effect over Wt-GATA2. Mean ± SEM of three independent analyses are shown.

32D cells, mature neutrophil counts and promyelocyte to neutrophil counts were significantly lower than those of Wt-GATA2-expressing 32D cells both after the 10-day and the 14-day cultures ($P=0.016$ and $P=0.0005$ after 10 days, and $P=0.009$ and $P=0.007$ after 14 days, respectively), indicating that p.A350_N351ins8-GATA2 impaired the G-CSF-mediated granulocytic differentiation (Fig. 4A and B). These morphological results were confirmed by the surface expression of CD11b after G-CSF stimulation (Fig. 4C). CD11b expression levels of p.R308P-GATA2-expressing 32D cells were the same as Wt-GATA2-expressing 32D cells, while that of p.A350_N351ins8-GATA2-expressing 32D cells was significantly lower than those of Wt-GATA2-expressing 32D cells on day 14 ($P=0.04$).

4. Discussion

In this study, we identified two novel *GATA2* gene mutations (p.R308P in the ZF-1 domain and p.A350_N351ins8 in the ZF-2 domain) in adult *de novo* AML patients. Most mutations in the ZF-2 domain of the *GATA2* gene are reportedly missense mutations.[8] Although three types of in-frame deletion mutations were reported, p.A350_N351ins8 mutation was firstly identified as an in-frame insertion mutation in the ZF-2 domain. L359V mutation, which was recurrently identified in CML-BC, increased transactivation activity and inhibited myelomonocytic differentiation and proliferation.[2] In contrast, T354M and T355del mutations, which were identified in families with hereditary MDS/AML, dominant-negatively reduced transactivation activity over Wt-GATA2.[3] However, it is notable that T354M-GATA2 inhibited the all-*trans* retinoic acid (ATRA)-induced granulocytic differentiation of HL-60 cells, but T355del-GATA2 did not. Consistent with the T354M mutation, p.A350_N351ins8 mutation reduced DNA-binding and transcriptional activities and impaired G-CSF-induced granulocytic differentiation of 32D cells. However, in contrast to T354M-GATA2, p.A350_N351ins8-GATA2 did not show a dominant-negative effect over Wt-GATA2 by transcriptional assay. Since p.A350_N351ins8 mutation was heterozygous in the clinical

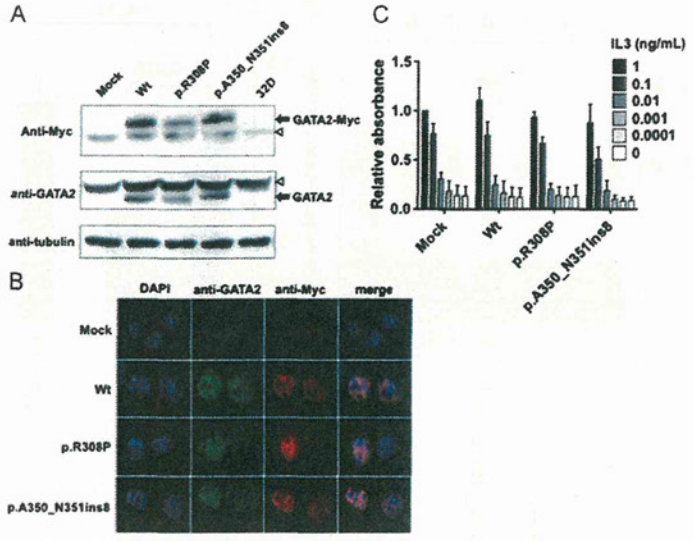

Fig. 3. Establishment of Wt- and Mt-GATA2-expressing 32D cells. (A) Stable expression of GATA2 protein in each cell line was confirmed by Western blotting using anti-Myc (upper panel) and anti-GATA2 (lower panel) antibodies. Of note is that no expression of endogenous GATA2 was observed in 32D cells. White arrowhead indicates non-specific band. (B) Immunofluorescence analysis showed the same localization of Wt- and Mt-GATA2. C. Ratio of cell viability of each GATA2-expressing 32D cell to mock-32D cells after 72-h culture at variable concentrations of IL3 is presented. Cell viability was measured using the CellTiter96 Proliferation Assay (Promega). Mean ± SEM of three independent analyses are shown. There was no significant difference of proliferation abilities between Wt- and Mt-GATA2-expressing 32D cells.

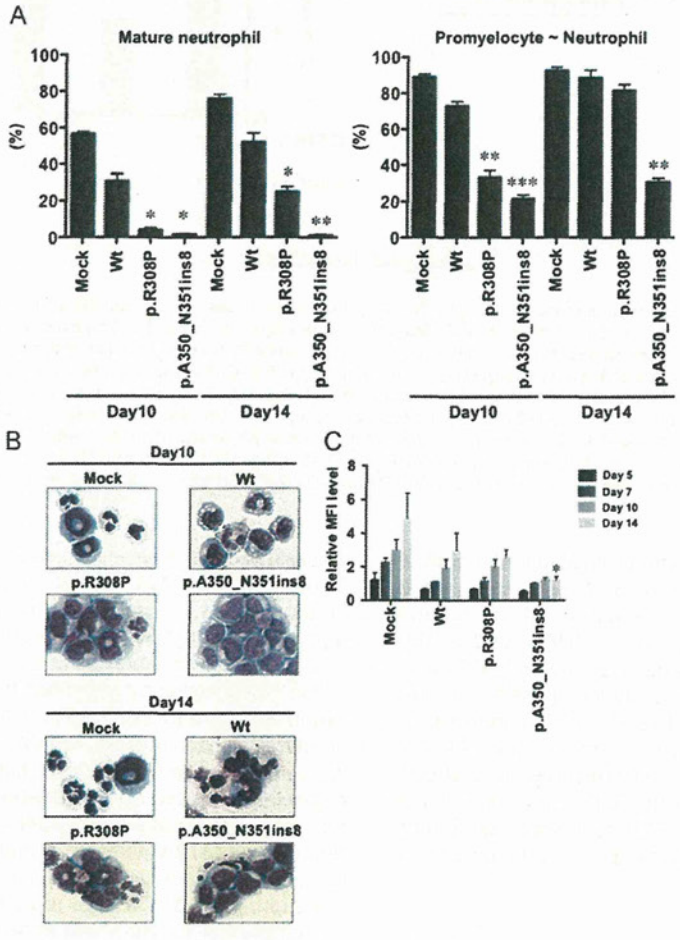

Fig. 4. G-CSF-induced granulocytic differentiation. (A) Granulocytic differentiation of G-CSF-treated 32D cells was morphologically determined. One hundred cells were counted in each experiment. Mean ± SEM of three independent analyses are shown. Mature neutrophil counts (left panel) and promyelocyte to neutrophil counts (right panel) on Day 10 and Day 14 were compared with Wt-GATA2-expressing 32D cells. (B) Morphological features of Wt- and Mt-GATA2-expressing 32D cells are shown. (C) The relative MFI level of CD11b to isotype after the G-CSF treatment in Mt-GATA2-expressing 32D cells were compared with Wt-GATA2-expressing 32D cells. Mean ± SEM of three independent analyses are shown. $^{*}P < 0.05$, $^{**}P < 0.01$, $^{***}P < 0.001$.